

MATHEMATICAL MODEL OF A MULTI-ROTOR DRONE PROTOTYPE AND CALCULATION ALGORITHM FOR MOTOR SELECTION

Mihai-Alin STAMATE^{1*}, Adrian-Florin NICOLESCU², Cristina PUPAZĂ²

¹⁾ PhD Student, Eng., Machines and Manufacturing Systems Department, University "Politehnica" of Bucharest, Romania

²⁾ Prof., PhD, Machines and Manufacturing Systems Department, University "Politehnica" of Bucharest, Romania

Abstract: This paper presents the theoretical stages for developing the mathematical model of a multirotor drone used for security applications and applicative works for development of the calculation algorithm necessary to determine the best choice of brushless motors which will equip the drone, based on the payload mounted onboard the drone and the specific mission that the drone is going to perform. First part of the paper presents the kinematics and dynamics modeling of the drone operation principles. It includes coordinates systems description, matrix description of roll-pitch - yaw individual and global rotation motions, as well as appropriate forces and torques acting on the drone system. Second part of the paper presents full calculation algorithm for motor selection, the procedure followed up to verify the resulted configuration for hexacopter's driving system as well as the virtual 3D prototype of the hexacopter achieved using SOLIDWORKS CAD software. Final aspects including electronic wiring and constructive - functional aspects related to hexacopter's on the board electronics are included too.

Key words: calculation algorithm, hexarotor drone, drone prototype, brushless motor, motor selection.

1. INTRODUCTION

The paper presents the solution of a hexarotor drone, adopted for designing and practical implementation. Following the elaborate calculation abstract and considering the experimental data obtained, the solution chosen, presented in this article, is a hexarotor in X model, given that this solution exhibits much higher air stability due to the resulting lift force created by the rotation of the six rotors (Fig. 1) [2, 6, 7, 8].

A multirotor UAV (unmanned aerial vehicle) is an unstable dynamical six-degree freedom system consisting of three-dimensional translation and rotational movements (3 dimensions). The translation motion is obtained by altering the direction and magnitude of the vertical traction force [2, 3, 4, 5].

For fixed rotor blades (relatively to those mounted on drones) the rotational movement for drone tilting is accomplished by individual variations of the rotor speeds to create rotation torques around the rotation center. The magnitude of the rotor speeds results in the magnitude of the traction force vector [2, 3, 4, 5].

The movement of the multi-rotor vehicle in two dimensions is illustrated in Figs. 2-4.

To analyze the behavior of the drone, two coordinate systems were used to represent the position and orientation of the hexacopter on the three dimensions, namely: the ground coordinate system and the hexacopter coordinate system [2, 3, 4, 7].

The ground coordinate system is a fixed reference system, so that, for example, if it is desired to define a

route the drone is to follow, this coordinate system will be used.

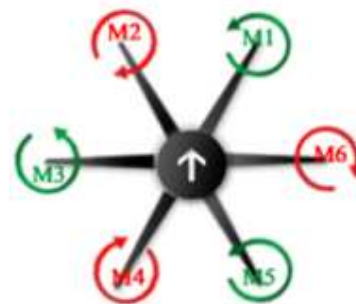


Fig. 1. Hexarotor in X, highlighting the rotational direction of the propellers and the direction of the drone (white arrow).

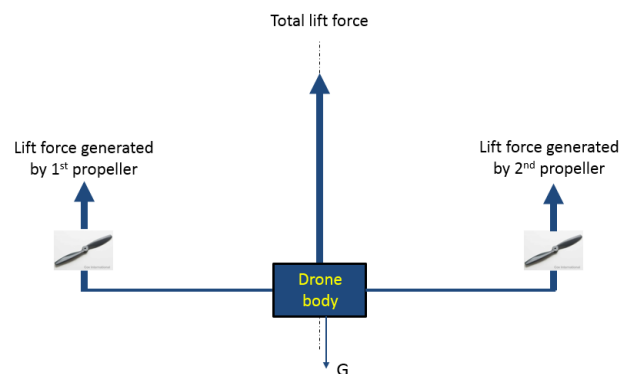


Fig. 2. The propellers rotate at the same angular velocity so that the total lift force vector is in the same direction as the force of gravity vector.

* Corresponding author: 313 Splaiul Independentei, district 6, Bucharest, Romania, Tel.: 0040 21 402 9369 E-mail addresses: stamyhay@yahoo.com (M.A. Stamate)

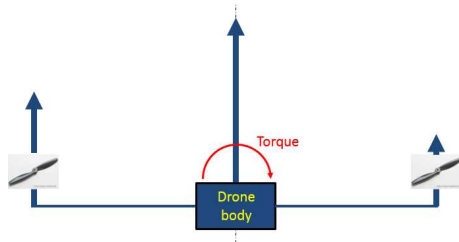


Fig. 3. By varying the speed of rotation of the propellers result in a torque of rotation.

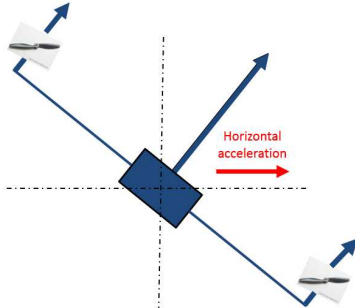


Fig. 4. The direction of the total thrust vector does not coincide with the direction of the gravitational force, resulting in a horizontal acceleration.



Fig. 5. The hexacopter coordinate system and numbering of the rotors.

The hexacopter coordinate system is chosen to be aligned with the drone mounted sensors, so that the x-axis will be oriented in the forward direction (the red mounting heads of the motors), the y-axis oriented to the left and the upward-facing axis, perpendicular to the plane determined by the axes x and y [2, 3, 4, 7] (Fig. 5).

Rotation axes. The attitude of the drone is defined as the orientation of the drone's coordinate system to the Earth's coordinate system. This represents the rotation of the drone around its x, y and z axes, in this case by using the right-hand rule, and consists of three movements: roll, pitch, and yaw (Fig. 6) [2, 4, 7].

The attitude is controlled by changing the speed of the motors, implicitly by the speed of rotation of the propellers, the rotors being numbered clockwise, with the rotor number 1 being in the right front position of the hexacopter (Fig. 5) [2, 4, 7].

The roll (roll) represents the rotation movement around the x axis, obtained by increasing / decreasing the speeds 1, 2 and 3, and simultaneously by increasing / decreasing the rotation speed of the rotors 4, 5 and 6. During this maneuver a torque of rotation around the x-axis and thus an angular acceleration occurs. The rotation angle for roll motion is noted with ϕ and is measured in rad/s [2, 4, 7].

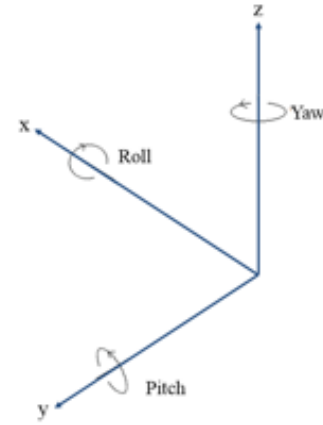


Fig. 6. The hexacopter rotation axes.

The pitch is the rotational movement around the y-axis and is achieved by increasing / decreasing the speed of the rotors 1 and 6 and simultaneously by increasing / decreasing the rotation of the rotors 3 and 4. Since the y-axis direction coincides with the position of the rotors 2 and 5, They do not affect the pitch. The pitch is noted with θ and is also measured in rad/s [2, 4, 7].

The yaw represents the rotation movement around the z axis. In the case of this movement, each propeller creates a torque around the z-axis when rotating. Thus, this torque is directed in the opposite direction to the rotation direction of the rotor. If the propeller rotates clockwise, it will create a trigonometric rotation around the z-axis [2, 4, 7].

To maintain a stable hexacopter, it is necessary to rotate the rotors in different directions so that the three rotors rotate clockwise and the other three in the trigonometric sense. The rotation movement is achieved by decreasing / increasing the speed of the rotors 1, 3 and 5 and simultaneously increasing/decreasing the rotation speed of the rotors 2, 4 and 6. The rotation angle for the rotation motion is noted with ψ [rad/s] [2, 4, 7].

Rotation matrices. The coordinate system of the ground and the coordinate system associated to the drone fuselage can be expressed to each other by a series of rotation matrices [7].

Yaw rotation matrix is

$$R_C^P(\psi) = \begin{bmatrix} \cos \psi & \sin \psi & 0 \\ -\sin \psi & \cos \psi & 0 \\ 0 & 0 & 1 \end{bmatrix}. \quad (1)$$

Pitch rotation matrix is

$$R_C^P(\theta) = \begin{bmatrix} \cos \theta & 0 & -\sin \theta \\ 0 & 1 & 0 \\ \sin \theta & 0 & \cos \theta \end{bmatrix}. \quad (2)$$

Roll rotation matrix becomes

$$R_C^P(\phi) = \begin{bmatrix} 1 & 0 & 0 \\ 0 & \cos \phi & \sin \phi \\ 0 & -\sin \phi & \cos \phi \end{bmatrix}. \quad (3)$$

By performing the three rotations, in the order presented above, the fuselage-ground rotation matrix is obtained:

$$R_C^P = R_C^P(\psi)R_C^P(\theta)R_C^P(\phi) = \begin{bmatrix} \cos\psi \cos\theta & \cos\psi \sin\theta \sin\phi - \sin\psi \cos\phi & \cos\psi \sin\theta \cos\phi + \sin\psi \sin\phi \\ \sin\psi \cos\theta & \sin\psi \sin\theta \sin\phi + \cos\psi \cos\phi & \sin\psi \sin\theta \cos\phi - \cos\psi \sin\phi \\ -\sin\theta & \cos\theta \sin\phi & \cos\theta \cos\phi \end{bmatrix}, \quad (4)$$

where R_C^P is an orthogonal matrix which means that its inverted matrix is equal to its transposed, so that the transformation of the ground – fuselage rotation matrix is done with the following relation:

$$(R_C^P)^{-1} = (R_C^P)^T = R_C^C. \quad (5)$$

Forces and moments. The two main forces which have impact on the drone during flight are: the force of gravity (G) and the traction force generated by the rotation of the rotors during rotation, by the entrainment of the air currents.

Also, against the multirotor acts the drag force, in the negative sense, with the tendency to oppose to the forward or upward movement of the drone [1, 2, 5].

Gravity. It will always have the direction along z axis and oriented downward, can be emphasized with the following expression:

$$F_{gravity}^C = R_C^C \begin{bmatrix} 0 \\ 0 \\ -mg \end{bmatrix} = \begin{bmatrix} mg \sin\theta \\ -mg \cos\theta \sin\phi \\ -mg \cos\theta \cos\phi \end{bmatrix}. \quad (6)$$

Lift. Traction represents the horizontal lifting force that allows the helicopter to fly horizontally and to hover at a stationary altitude in the air. This force depends on the sum of the revolutions of the six rotors that sustain the drone. To control the total traction force, the rotation of certain rotors varies by increasing the rotation of a specific number of rotors (usually 3) while reducing the rotation of the other rotors during the rotation or pitch maneuvers. Since the rotors are fixed, the total traction force generated by the six rotors will have the direction in the z -axis direction (if we use the coordinate system associated with the drone as reference) and the upward-facing direction. During this hovering maneuver, this traction force can be approximated by the equation:

$$F_{traction}^C = b \sum_{i=1}^6 \Omega_i^2, \quad (7)$$

where b is traction force constant, in Ns^2 .

Forward opposing force. During flight, a forward-facing force pushes against the fuselage (frame) of the drone. This force will affect the accelerations on x and y , and it can be expressed, during the flight maneuver at constant altitude, by the equation below:

$$F_{oppo \sin gforce}^C = \begin{bmatrix} -\mu u \\ -\mu v \\ 0 \end{bmatrix}, \quad (8)$$

where μ – constant in $\frac{kg}{s}$; u – linear velocity along x axis (referenced to fuselage); v – linear velocity along y axis (referenced to fuselage).

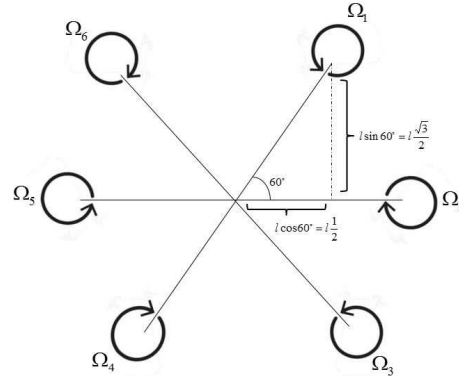


Fig. 7. Distance of the rotors relative to drone center of gravity.

Drag. Drag force is the force created by air resistance against the drone fuselage and it is proportional to the square of the speed, shape and size of the object, according to the following relation:

$$F_{drag}^C = \begin{bmatrix} -\frac{1}{2} CA_x \rho u |u| \\ -\frac{1}{2} CA_y \rho v |v| \\ -\frac{1}{2} CA_z \rho w |w| \end{bmatrix}, \quad (9)$$

where C is friction constant, A_l – cross section area in m^2 , ρ – air density in kg/mm^3 , w – linear velocity along z axis (referenced to fuselage).

Torques (moments). As mentioned above, rotation speeds around the x , y and z axes can be obtained by varying the rotational speed of the rotors, resulting in the yaw, roll, and pitch maneuvers.

The moment of force, defines the product of force and arm of force, so that the rotors will influence the rotation of the drone after a certain axis according to the force arm (the relative distance of each relative to the center of gravity of the drone).

Figure 7 shows the lengths and angles of the support arms of the motors relative to the center of gravity of the drone, which represents the distance from the rotor to the axis of rotation, where Ω [rad/s] is the propeller rotational speed, l [m] is the length of the support arm of the propeller-motor assembly and d [Nms²] is a forward-resistance factor.

Roll torque (moment). By decreasing $\Omega_1, \Omega_2, \Omega_3$ and increasing $\Omega_4, \Omega_5, \Omega_6$ will result a positive roll torque.

$$\tau_{roll} = bl(-\Omega_2^2 + \Omega_5^2 + \frac{1}{2}(-\Omega_1^2 - \Omega_3^2 + \Omega_4^2 + \Omega_6^2)). \quad (10)$$

Pitch torque (moment). By decreasing Ω_1, Ω_6 and increasing Ω_3, Ω_4 will result a positive pitch moment.

$$\tau_{pitch} = bl \frac{\sqrt{3}}{2} (-\Omega_1^2 + \Omega_3^2 + \Omega_4^2 - \Omega_6^2). \quad (11)$$

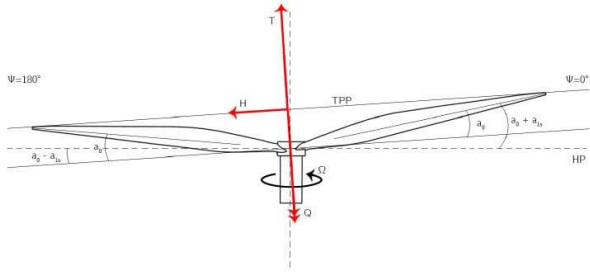


Fig. 8. Forces and moments that act on a propeller during rotation.

Yaw torque (moment). By decreasing $\Omega_1, \Omega_3, \Omega_5$ and increasing $\Omega_2, \Omega_4, \Omega_6$ will result a positive yaw moment,

$$\tau_{yaw} = d(-\Omega_1^2 + \Omega_2^2 - \Omega_3^2 + \Omega_4^2 - \Omega_5^2 + \Omega_6^2). \quad (12)$$

Gyroscopic effect of the propeller. The rotation of the propellers results in production of a gyroscopic effect defined by the following expression:

$$\tau_{gyro} = \begin{bmatrix} -J_r \Omega_r \dot{\theta} \\ J_r \Omega_r \dot{\phi} \\ 0 \end{bmatrix}, \quad (13)$$

$$\Omega_r = -\Omega_1 + \Omega_2 - \Omega_3 + \Omega_4 - \Omega_5 + \Omega_6, \quad (14)$$

where J_r - inertial moment of the propeller, measures in [Nms²]; Ω_r - total rotational velocity of the propellers [rad/s].

Rotor dynamics. A rotor generates three types of forces and moments during rotation around its own axis: the lift force, a horizontal force and a moment of resistance (Fig. 8).

The lift force acts perpendicular to the plane determined by the Tip Path Plane (TPP). It has the expression:

$$T = C_T \rho A R^2 \Omega^2, \quad (15)$$

where T - traction force (lift); C_T - lift coefficient; ρ - air density [kg/m³]; A - area of the disk described by the rotor [m²]; R - rotor radius; Ω - angular velocity of the rotor [rad/s].

The horizontal force (forward resistance) is the force parallel to the plane described by the propeller wingtips. This force is non-existent during hovering or axial flight maneuvers. Its expression is:

$$H = C_H \rho A R^2 \Omega^2, \quad (16)$$

where H - drag; C_H - drag coefficient.

Resistant torque Q acts perpendicularly to the plane described by the wingtips of the propeller, its direction being dictated by the propeller direction of rotation. It has the expression:

$$Q = C_Q \rho A R^3 \Omega^2, \quad (17)$$

where Q - resistant torque; C_T - resistant torque coefficient

Geometrical elements of the propeller

Propeller diameter D represents the diameter of the disk created by the rotation of the blades, $D = 2R$.

The central part, the propeller hub does not produce lift and it is usually covered by an aerodynamic profile, named crest. The propeller area A_{el} is the area of its disk:

$$A_{el} = \frac{\pi \cdot D^2}{4}. \quad (18)$$

Global fill coefficient σ_{el} represents the ratio between the projection of the blade surface on the propeller disk and the propeller surface, Eq. (19), where z is the number of blades and S_p is the surface of a blade. The number of blades of a rotor may vary from two blades to five blades. Since, in general, the propeller string, c , is variable across the radius, a local fill coefficient, Eq. (20), is defined as follows:

$$\sigma_{el} = \frac{z \cdot S_p}{A_{el}}, \quad (19)$$

$$\sigma = \frac{z \cdot c}{2} \cdot \pi \cdot r, \quad (20)$$

where r - current radius where we will find the blade element with a c string.

Geometric pitch of the propeller H represents the distance measured along the rotation axis of the propeller which, theoretically, any of the blade elements can travel at a complete rotation. For illustration, we take into consideration the fact that by developing the cylinder with H height and having the axis superimposed over the axis of the propeller and tangent to the blade tips, a rectangle with a base whose diagonal is precisely the length traveled by the blade tip at a rotation of the propeller, that is, the curve unfolded in plan. Correctly, the angle formed between the diagonal of the rectangle and its base is called the pitch angle (Fig. 9).

2. ALGORITHM FOR MOTOR SELECTION

The calculation algorithm for haxacopter motor selection includes as main specific steps:

1. Preliminary data definition / fixed values for functional parameters settings.
2. Calculation of battery capacity capacity in Ah, based on flight time and motor speed factor Kv .
3. Calculation of lost motor rpm, based on voltage based on voltage.
4. Calculation of aerial speed (tangential speed).
5. Calculation of geometric pitch angle of the propeller.
6. Calculation of lift force, drag and traction force
7. Calculation of motor power.

Detailed calculation parameters and specific formulas are listed in Table 1.

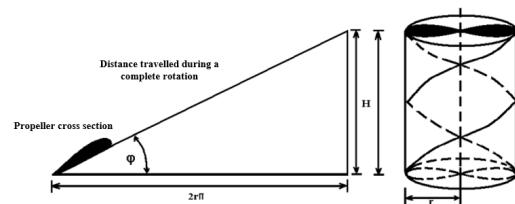


Fig. 9. Geometric pitch of the propeller H .

Table 1

Calculation algorithm for motor selection

Preliminary data	
Motor parameter in rpm, at a tension of 1V	$K_v = 620 \frac{1}{V \cdot \text{min}}$
Maximum current voltage, input to motor [V]	$U_{\max} = 14.8 V$
Maximum current intensity, input to the motor [A]	$I_{\max} = 17.5 A$
Actual current voltage input to the motor [V]	$U_I = 14.8 V$
Actual current intensity, input to the motor [A]	$I_i = 14 A$
Internal resistance of the spindle [Ohm]	$R_s = 0.126 \Omega$
Flight time of the hexarotor [s]	$t = 480 s$
% of the engines running	$x = \frac{60}{100}$
Propeller pitch [m]	$H_{pas} = 13 \text{ in} = 0.3302 m$
Number of propeller blades	$n = 2$
Air density [kg/m ³] at sea level and 15°C	$\rho = 1.225 \frac{\text{kg}}{\text{m}^3}$
Air density at 100 m altitude	$\rho_H = 1.225 \left(1 - \frac{100}{44308}\right)^{4.2253} = 1.2134$
Propeller diameter [m]	$D = 13 \text{ in}$
Blade radius [m]	$R_b = \frac{D}{2} = 0.1651 m$
Lift calculation radius (without the hub)	$R_p = R_b - 0.006 m = 0.1591 m$
Reference radius	$r = \frac{2}{3} R_p = 0.1061 m$
Profile string	$c_{profil} = 0.034 m$
Area of one propeller [m ²]	$S_p = R_p \cdot c_{profil} = 0.0054 m^2$
Area of the entire rotor	$A_{rotor} = \pi \cdot R_p^2 = 0.0795 m^2$
Global fill coefficient	$\sigma_{el} = n \cdot \frac{S_p}{A_{rotor}} = 0.1360$
Approximate mass of the hexarotor (with the payload installed)	$G = mass \cdot g = 26.4780 N$
Mass one motor can lift with a 13in propeller installed on it	$\exp_{mass} = 1.58 \text{ kg}$
Calculation of battery capacity in Ah, based on flight time and K	
Current power of one motor	$P = U_i \cdot I_i = 207.2 W$
Battery capacity needed for flight [Ah]	$Capacity = \frac{6}{3600} \cdot \frac{P \cdot t}{U_i} \cdot x$
Calculation of lost motor rpm, based on voltage	
Ideal rpm	$rpm_{ideal} = K_v \cdot U_i$
Lost voltage	$U_p = R_s \cdot I_i$
Lost power on spool coil	$P_s = R_s \cdot I_i^2$
Real rpm	$rpm_{real} = K_v \cdot (U_i - U_p)$
Lost rpm	$T_p = K_v \cdot I_i \cdot R_s$
Real maximum rpm	$rpm_{\max \text{ im. real}} = 17976 rpm$

Table 1 (Continuation)

Calculation of aerial speed (tangential speed)	
Revolutions per second	$rps_{real} = rpm_{real} = 134.7053rps$
Angular speed [radian/s]	$\omega = rps_{real} \cdot 2 \cdot \pi$; $\omega_{max\,im} = rpm_{max\,im,real} \cdot 2 \cdot \pi$
Tangential speed at propeller wingtip	$v_{tan\,g,at.wingtip} = \omega \cdot R_p$
Tangential speed at reference radius	$v_{tan\,g} = \omega \cdot r$
Dynamic air viscosity	$\mu = 1 \cdot 10^{-5} \frac{kg}{m \cdot s}$
Calculation of geometric pitch angle of the propeller	
Geometric pitch angle calculation using ideal geometric pitch	$\phi = a \tan\left(\frac{H_{pas}}{2\pi \cdot 0.75 \cdot R_b}\right)$; $\phi_{real} = 6\,deg = 0.1047rad$
Calculation of lift force	
Lift coefficient at a 10-degree incidence angle	$C_L = 0.98$
Lift generated by a single motor	$L_{rotor} = \frac{1}{2} \cdot \rho \cdot V_{tan\,g}^2 \cdot S_p \cdot C_L$
Total mass that can be lifted by the hexarotor	$m_{rotor} = 6 \cdot \frac{L_{rotor}}{g}$
Calculation of drag	
Drag coefficient at a 10-degree incidence angle	$C_D = 0.09$
Drag generated by one rotor	$Drag = \frac{1}{2} \cdot \rho \cdot V_{tan\,g}^2 \cdot S_p \cdot C_D$
Calculation of traction force	
Traction coefficient	$C_T = \frac{G}{6 \cdot \rho \cdot A_{rotor} \cdot (\omega \cdot R_p)^2}$
Traction needed for one motor	$Traction = C_T \cdot \rho \cdot A_{rotor} \cdot (\omega \cdot R_p)^2$
Calculation of power	
Maximum available power for one motor	$P_{max\,av} = 207\,W$
Total resistance coefficient	$C_X = C_D \cdot (1 + C_L^2)$
Power coefficient	$C_P = C_T \cdot \sqrt{\frac{C_T}{2}} + \sigma_{el} \cdot \frac{C_X}{8}$
Maximum mechanical power needed for the entire hexarotor	$P_{nec} = \rho \cdot A_{rotor} \cdot (\omega \cdot R_p)^3 \cdot C_P$

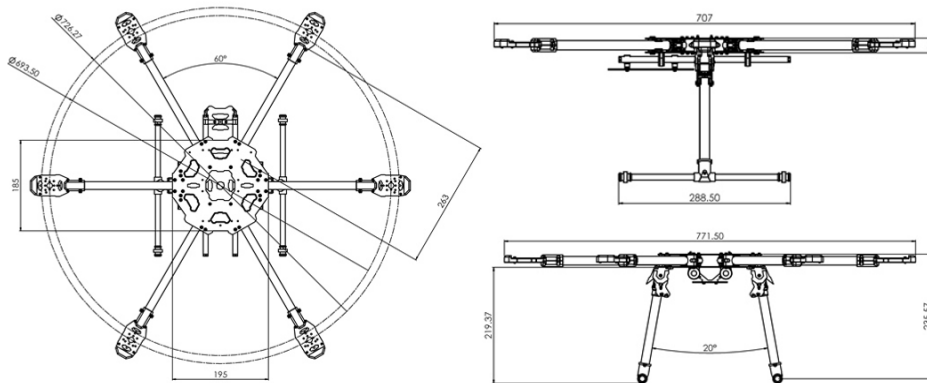


Fig. 10. The hexarotor dimensions.

The hexacopter prototype. The above presented calculations, correlated with another set of calculations (which are not presented in this paper) were developed to analyze the drone in all flight modes (hover, ascending flight, forward flight, rotation around the center axis, lateral flight).

Also, the calculations were correlated with the data obtained and checked using the platform on the website www.ecalc.ch, which allows, based on the user’s inputs, to verify if the chosen version of the drone is correct, to be able to fly without errors [1].

Figure 10 presents the main hexacopter dimensions (2D drawings created with SOLIDWORKS CAD software).

The virtual 3D hexacopter prototype was realized using SOLIDWORKS CAD software (Figs. 11 and 12).

Figure 12 illustrates the fully equipped PROTOTYPE of the hexacopter including: 13" carbon fiber propellers, brushless motors, 4S LiPo battery, ESCs (Electronic Speed Controller), main controller, gimbal, camera, PMU (Power Module Unit), GPS antenna and receiver [6].

Figures 13–17 illustrate the data obtained from the simulations performed on the www.ecalc.ch platform, using the chosen variant of the equipment mounted on the hexacopter, to identify any inconsistencies or errors that may occur during the flight of the hexarotor [1].



Fig. 11. The CAD prototype of the hexacopter.

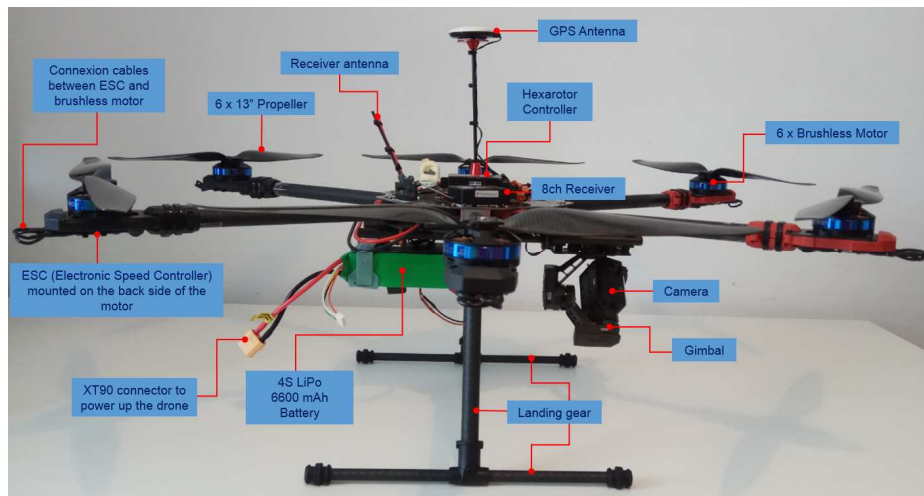


Fig. 12. Hexacopter PROTOTYPE fully equipped.



Fig. 13. Choosing the components that equip the drone [1].


Remarks:		Motor @ Optimum Efficiency	Motor @ Maximum	Motor @ Hover	Total Drive	Multicopter
Battery	Load: 19.44 C	Current: 8.44 A	Current: 19.44 A	Current: 4.09 A	Drive Weight: 1430 g	All-up Weight: 2845 g
	Voltage: 13.03 V	Voltage: 13.96 V	Voltage: 12.87 V	Voltage: 14.39 V	Drive Weight: 50.4 oz	All-up Weight: 100.4 oz
	Rated Voltage: 14.80 V	Revolutions*: 7941 rpm	Revolutions*: 6331 rpm	Revolutions*: 3504 rpm	Thrust-Weight: 2.6 : 1	add. Payload: 3483 g
	Energy: 88.8 Wh	electric Power: 117.8 W	electric Power: 250.3 W	Throttle (log): 36 %	Current @ Hover: 24.53 A	Current @ Hover: 122.9 oz
	Total Capacity: 6000 mAh	mech. Power: 99.0 W	mech. Power: 192.3 W	Throttle (linear): 47 %	P(in) @ Hover: 363.0 W	max Tilt: 63 °
	Used Capacity: 5100 mAh	Efficiency: 84.0 %	Power-Weight: 527.8 W/kg	electric Power: 58.8 W	P(out) @ Hover: 275.2 W	max. Speed: 45 km/h
	min. Flight Time: 2.6 min		239.4 W/lb	mech. Power: 45.9 W	Efficiency @ Hover: 75.8 %	28 mph
	Mixed Flight Time: 9.0 min		Efficiency: 76.8 %	Power-Weight: 127.6 W/kg	Current @ max: 116.66 A	est. rate of climb: 8.5 m/s
	Hover Flight Time: 12.5 min		est. Temperature: 50 °C	57.9 W/lb	P(in) @ max: 1726.5 W	1673 ft/min
	Weight: 568 g		122 °F	Efficiency: 77.9 %	P(out) @ max: 1153.7 W	Total Disc Area: 51.38 dm ²
	20 oz		Wattmeter readings	est. Temperature: 31 °C	Efficiency @ max: 66.8 %	796.39 in ²
			Current: 116.64 A	88 °F		with Rotor fail: 
			Voltage: 13.03 V	specific Thrust: 8.06 g/W		
			Power: 1519.8 W	0.28 oz/W		

Fig. 14. Verifying the actual configuration [1] (the green circle with white check mark indicates that the actual configuration has been properly chosen).

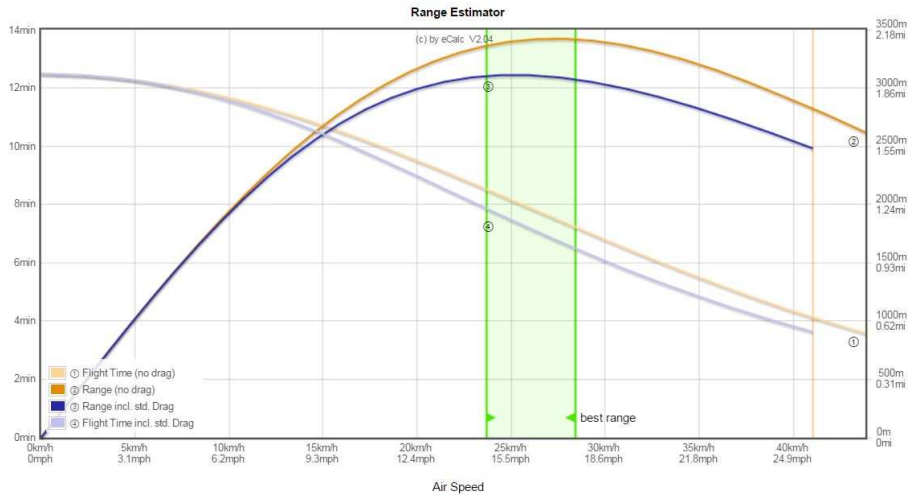


Fig. 15. Hexacopter range estimator [1].

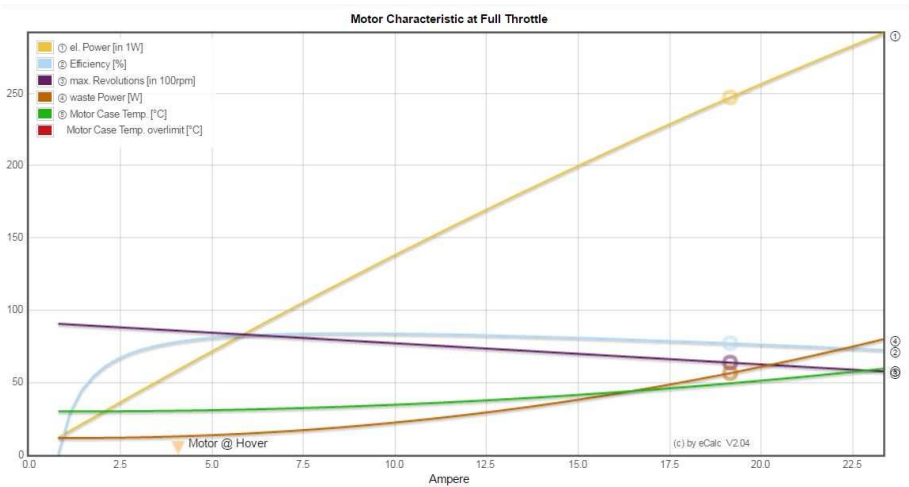


Fig. 16. Brushless motor characteristics at full throttle [1].

Prop-Kv-Wizard

All-up Weight: g

of Rotors:

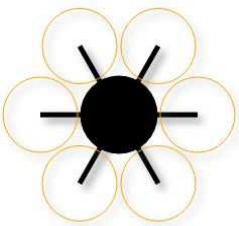
Frame Size: mm

Battery - Rated Voltage: V

Propeller - Diameter: inch max. 13.6"

Propeller - Pitch: inch max. 8.6"

Propeller - # Blades:



recommended KV: **460 ... 670** rpm/V

min. Motor Power: **250 ... 435** W+

min. ESC size: **20 ... 35** A+

Fig. 17. Choosing the right motor-propeller combination [1].

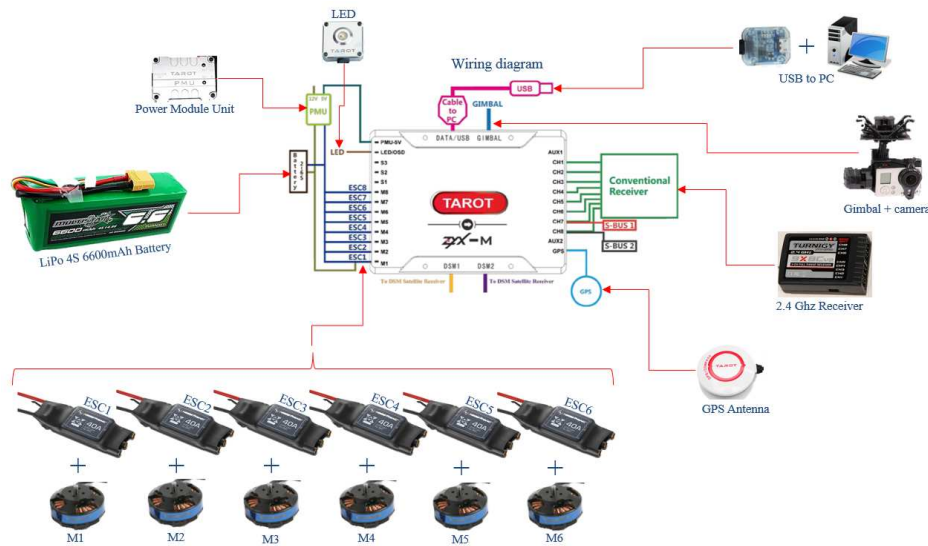


Fig. 18. Wiring diagram.

Constructive-functional aspects of the hexarotor

Figure 18 shows the wiring diagram, where the connection of the avionics components is highlighted. They connect to the central element of the hexarotor – the main controller, which provides the processing power required for the evolution of the drone during flight and is equipped with intelligent computing and navigation control systems, 32-bit processor, integrated anti-vibration sensor, metal housing, supports dual S-BUS reception, sends warnings in case of failure.

Power is provided by a 4S LiPo battery pack with a capacity of 6600 mAh, voltage – 14.8V. From the battery (indicated on the Battery 2-6S circuit diagram), a fraction of the voltage is distributed through the upper plate (which also acts as the voltage distribution board) to the 6 Electronic Speed Controllers (ESC), which, in turn, through the engine control software distributes the voltage to brushless electric motors.

The other fraction of the voltage supplied by the battery passes through the power distribution module (PMU) from where it is divided into 2 bus lines: the 5V bus provides the voltage required for the main controller (coupled to the PMU-5V slot) and the other, a 12-volt bus system provides power to the gimbal-camera system. For the 3-axis gimbal control part, the gimbal cable is inserted into the gimbal slot on the controller.

Engine control is achieved by coupling servo cables to the M1-M6 ports on the controller (corresponding to the 6 ESCs). At the other end of the controller, the servo cables are inserted into the appropriate CH1-CH8 slots, and the opposite end of the servo cables is inserted into the slots on the receiver.

In the case of the hexarotor, the control of the motors is made through channel 3 on the receiver.

The GPS antenna connects to the GPS slot on the controller. To program the different flight modes and set the control limits on the 3 axes: pitch, roll, rotation, via a USB cable, the drone is connected to the PC and the software can be programmed (on the pink cable scheme - Cable to PC). To indicate the operation modes with the help of light signals, a LED unit has been installed, connecting it to the LED / OSD slot on the controller. Optionally, if a FPV – First Person View system is

installed, it will require an OSD – On Screen Display equipment, which will also connect to the LED / OSD slot on the controller.

In the following, the components used for the practical realization of the above mentioned hexarotor solution are briefly presented.

For the frame side, carbon fiber tubes were used, like the landing gear arms for engine mounts due to the reduced weight of the material. As a support of the above-mentioned arms, landing gear and avionics and camera equipment, two carbon fiber plates (upper and lower) were used, which are assembled with screws. After checking the obtained data, the next step was to equip the drone, as shown in the following lines. For propulsion, the hexarotor was equipped with Tarot 4006/620KV brushless electric motors. To control the engine start/stop phases, speed and rotating direction ESCs (Electronic Speed Controller) were mounted at the bottom side of the motors. The type of the ESC chosen is Hobbywing XRotor 40A-OPTO.

To produce lift 13" carbon fiber propellers, Tarot 1355 type, were used, and as a power source the hexarotor was equipped with a 4 cell LiPo 6600 mAh battery, Multistar 6600mAh Lipo type.

For the avionics part, the drone was equipped with a main controller (the central component that also provides the automatic pilot function and controls the flight modes of the drone), Tarot ZXY-M model, a GPS antenna, a voltage distribution module, to supply power from battery to consumers, a USB module to program the drone, and, of course, the Tx-Rx radio frequency transmission equipment pack, Turnigy TGY 9x model.

Considering the purpose of this hexacopter, namely, perimeter surveillance, it is mandatory to equip the drone with a surveillance camera. For this purpose, it was used a 3-axis steering and position control system from an integrated Tarot T4-3D controller. Surveillance is achieved with a Turnigy Action Cam video camera, which can shoot at a resolution of 1080 p, and its autonomy is ensured by a battery.

As an auxiliary solution, the drone can be equipped with infrared surveillance camera (FLIR – Forward Looking Infrared) or thermal imaging camera for

surveillance in difficult visibility conditions (at night or in dense conditions).

3. CONCLUSIONS

The mechanical structure of the hexarotor, the the elaborate calculation abstract which shows the behavior of the drone during various flight maneuvers (hover flight, forward flight, lateral flight, ascensional flight, rotation around the vertical axis), the number and type of the mototrs that equip the drone, depending on the payload to be mounted on the hexarotor, as well as integration of the avionics components and Tx remote control, represent original contributions to this work.

From a cost point of view, compared to a similar constructive-functional solution available on the market at a price of approximately EUR 3,800 - 4500, the solution presented in this article has a final price of about EUR 1,500, by cumulating the price of the components that equip the drone, the materials and tools used for construction. Thus, one may conclude that this drone represents an acceptable financial solution to be used in perimeter securing applications, for the surveillance of industrial facilities of strategic interest, government buildings, detention centers, borders, illegal border crossing.

REFERENCES

- [1] *Drone configuration calculation, range estimator, motor characteristic at full throttle*, available at: <https://www.ecalc.ch/xcoptercalc.php>.
- [2] V. Artale; C.L.R. Milazzo; A. Ricciardello, *Mathematical Modeling of Hexacopter*, Appl. Math. Sci, Vol. 7, No.97, 2013, pp. 4805–4811.
- [3] J. Gordon Leishman; *Principles of Helicopter Aerodynamics*, Cambridge University Press, 2000.
- [4] C. Månsson, D. Stenberg, *Model-based Design Development and Control of a Wind Resistant Multirotor UAV*, Department of Automatic Control, Lund University, 2014.
- [5] V. Martínez, *Modeling of the Flight Dynamics of a Quadrotor Helicopter*, A MSc Thesis in Cranfield University, Vol. 71, No. 2, 2007, pp. 149–438.
- [6] Aeroquad: The open source quadcopter / multicopter, available at: <http://aeroquad.com/>.
- [7] R. Leishman, J. Macdonald, T. McLain, R. Beard, *Relative navigation and control of a hexacopter*, in *Robotics and Automation (ICRA)*, 2012 IEEE International Conference, pp. 4937–4942.
- [8] Gabriel M. Hoffmann, Haomiao Huang, Steven L. Waslander, C. J. Tomlin, *Quadrotor helicopter flight dynamics and control: Theory and experiment*, Proc. of the AIAA Guidance, Navigation, and Control Conference, Vol. 2, p. 7, 2007.